

# ATP-2 Interacts with the PLAT Domain of LOV-1 and Is Involved in *Caenorhabditis elegans* Polycystin Signaling

Jinghua Hu and Maureen M. Barr\*

Division of Pharmaceutical Sciences, School of Pharmacy, University of Wisconsin-Madison, Madison, WI 53705

Submitted September 29, 2004; Revised November 10, 2004; Accepted November 16, 2004  
Monitoring Editor: Martin Chalfie

*Caenorhabditis elegans* is a powerful model to study the molecular basis of autosomal dominant polycystic kidney disease (ADPKD). ADPKD is caused by mutations in the polycystic kidney disease (*PKD1* or *PKD2*) gene, encoding polycystin (PC)-1 or PC-2, respectively. The *C. elegans* polycystins LOV-1 and PKD-2 are required for male mating behaviors and are localized to sensory cilia. The function of the evolutionarily conserved polycystin/lipoxygenase/ $\alpha$ -toxin (PLAT) domain found in all PC-1 family members remains an enigma. Here, we report that ATP-2, the  $\beta$  subunit of the ATP synthase, physically associates with the LOV-1 PLAT domain and that this interaction is evolutionarily conserved. In addition to the expected mitochondria localization, ATP-2 and other ATP synthase components colocalize with LOV-1 and PKD-2 in cilia. Disrupting the function of the ATP synthase or overexpression of *atp-2* results in a male mating behavior defect. We further show that *atp-2*, *lov-1*, and *pkd-2* act in the same molecular pathway. We propose that the ciliary localized ATP synthase may play a previously unsuspected role in polycystin signaling.

## INTRODUCTION

Autosomal dominant polycystic kidney disease (ADPKD) is one of the most common monogenic diseases, affecting one per 400–1000 individuals (Igarashi and Somlo, 2002). This syndrome is characterized by progressive development of fluid-filled, epithelial cysts in the kidney, liver, and pancreas and accounts for ~10% of all cases of end-stage renal disease. Mutation in either the polycystic kidney disease (*PKD1* or *PKD2*) gene accounts for 95% of all ADPKD cases. *PKD1* encodes polycystin (PC)-1, a 4302-amino acid protein with a large extracellular domain, a G protein-coupled receptor proteolytic site (GPS), 11 predicted transmembrane (TM) domains, and an intracellular C terminus. The polycystin/lipoxygenase/ $\alpha$ -toxin (PLAT) domain is located in the first cytoplasmic loop between TM1 and TM2 and has been postulated to be involved in membrane-protein or protein-protein interactions (Batesman and Sandford, 1999). This domain is conserved in all PC-1 family members and also found in a variety of membrane- or lipid-associated proteins. Polycystin-2 (PC-2, encoded by *PKD2*) shares homology with the transient receptor protein (TRP) channels and acts as a nonselective cation channel. Defects in PC-1 or PC-2 signaling may result in epithelial dedifferentiation and cyst formation. Several signaling pathways regulated by PC-1 and PC-2 have been identified using *in vitro* approaches, including G protein signaling, JAK/STAT cell cycle regulation, and mechanotransduction (Boletta and Germino, 2003), but the physiological relevance to normal and disease states remains unclear.

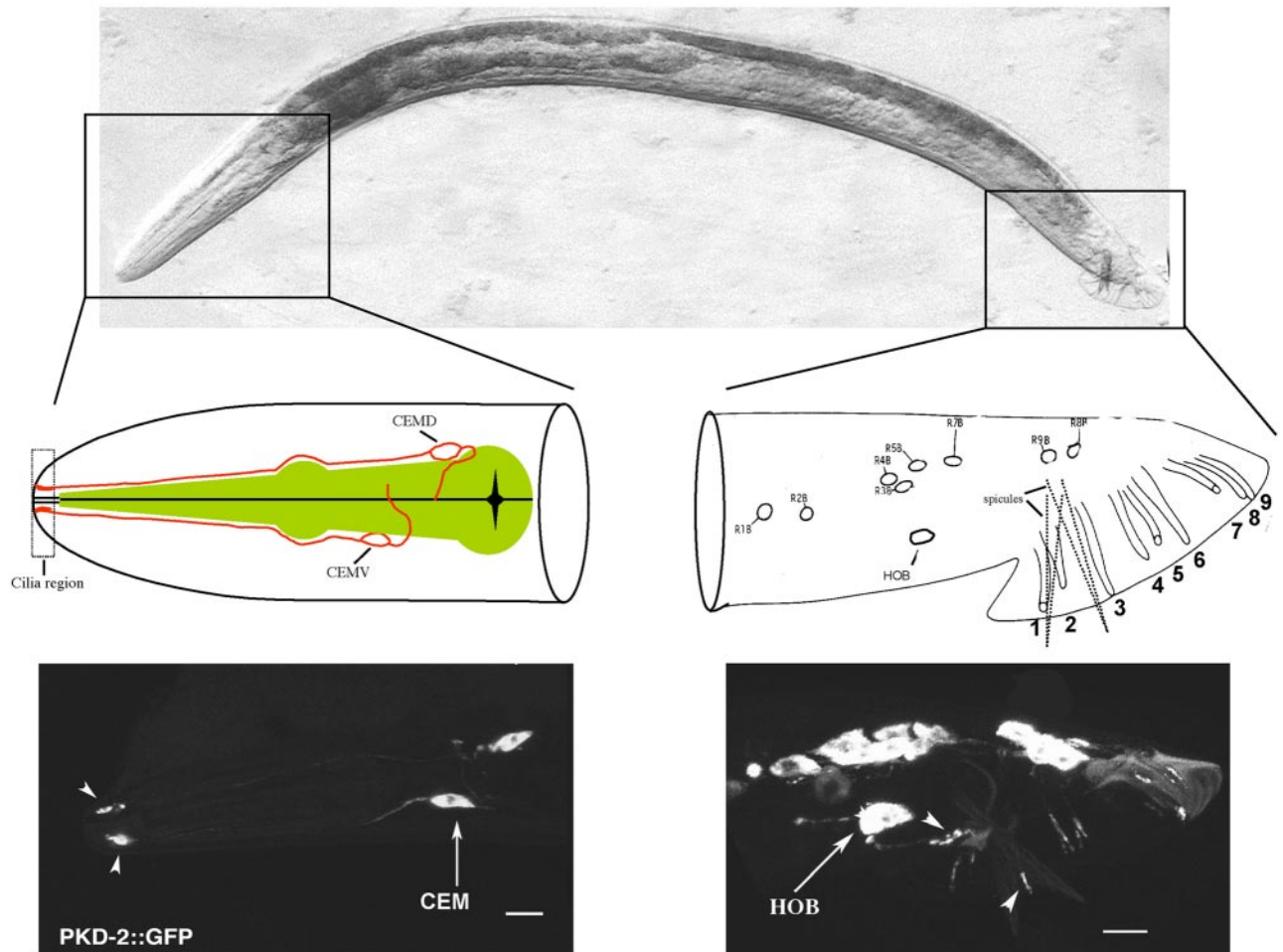
The nematode *C. elegans* is a simple but powerful animal model for studying basic molecular mechanisms underlying human ADPKD. The *C. elegans* LOV-1 and PKD-2 proteins are homologues of human PC-1 and PC-2 (Barr and Sternberg, 1999; Barr *et al.*, 2001). *lov-1* (location of vulva) and *pkd-2* act nonredundantly in the same genetic pathway and are required for two male mating behaviors, response to hermaphrodite contact and vulva location. Accordingly, *lov-1* and *pkd-2* are exclusively expressed in three categories of adult male sensory neurons: the rays, the hook, and the head cephalic (CEMs), which mediate response, vulva location, and potentially other male-specific sensory behaviors, respectively (Figure 1a). LOV-1 and PKD-2 localize to the cilia of these male-specific sensory neurons. Ciliary localization of polycystins is critical for polycystin function and observed in a diversity of species ranging from *C. elegans* to human (Igarashi and Somlo, 2002; Watnick and Germino, 2003). LOV-1 shares a similar architecture with other PC-1 family members: a large extracellular domain (although there is no primary sequence homology between the extracellular regions of LOV-1 and PC-1), a GPS site, 11 TM domains, and the intracellular PLAT domain. Like PC-1 and PC-2, the cellular functions of LOV-1 and PKD-2 remain elusive. Based on PLAT sequence homology, a nonredundant genetic PKD pathway, and PC ciliary subcellular localization in both *C. elegans* and mammals, we hypothesize that the PLAT domain may perform an evolutionarily conserved role in mediating PC-1 intracellular signaling pathways.

In this work, we find that overexpression of the LOV-1 PLAT domain in transgenic *C. elegans* results in male mating behavior defects. To identify regulators or targets of LOV-1 PLAT domain, we performed a yeast two-hybrid (Y2H) screen. ATP-2 is identified as one candidate that physically interacts with the PLAT domain. We demonstrate that the  $\beta$  barrel domain of ATP-2 is responsible for this interaction. ATP-2 and other ATP synthase components were found to localize to the cilia of male-specific sensory neurons. Over-

Article published online ahead of print in *MBC in Press* on November 24, 2004 (<http://www.molbiolcell.org/cgi/doi/10.1091/mbc.E04-09-0851>).

\* Corresponding author. E-mail address: mmbarr@pharmacy.wisc.edu.

**a**



**b**

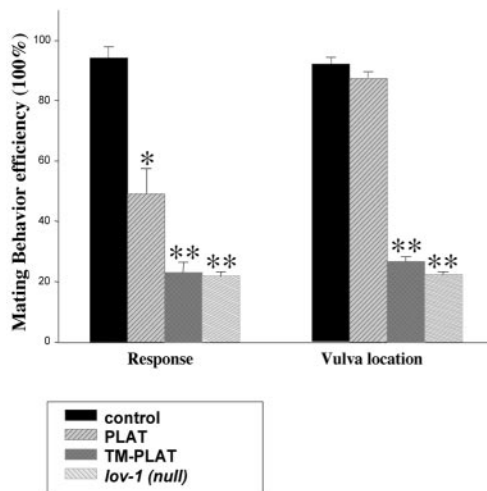


**Figure 1.** Overexpression of the PLAT domain in male-specific neurons interferes with LOV-1 function. (a) Top, differential interference contrast side view image of an adult *C. elegans* male oriented head (left) to tail (right). Middle and bottom, PKD-2::GFP is expressed in male head CEM neurons (left) and tail ray RnB and hook HOB neurons (right). Middle left, cilium, dendrite, cell body, and axon of the dorsal CEM (CEMD) and ventral CEM (CEMV) neuron are drawn in the male head diagram. CEMD and CEMV are arranged as left-right pairs (one side shown here). Cilia are in the nose region (dashed rectangular box). The pharynx is colored green. Middle right, positions of nuclei of all *lov-1*- and *pkd-2*-expressing cells in the *C. elegans* adult male tail, modified from Sulston *et al.* (1980). Ray neurons are arranged as left-right bilateral pairs (one side shown here). The male tail has nine bilaterally arranged rays (numbered 1–9, anterior to posterior) required for response and turning behaviors (Liu and Sternberg, 1995). HOB is an asymmetric ciliated hook neuron that mediates vulva location behavior (Liu and Sternberg, 1995). The copulatory spicules are indicated by dotted lines. Bottom, PKD-2::GFP localization in the *C. elegans* adult male head (left) and tail (right). Arrowheads indicate cilia and arrows identify neuron cell body. (b) Overexpression of the LOV-1 PLAT domain in wild-type males leads to defects in mating behavior. A 1.3-kb *pkd-2* promoter was used to drive expression of the PLAT domain, PLAT (amino acids 2112–2302), or the first LOV-1 transmembrane domain followed by the PLAT domain, TM-PLAT (amino acids 2083–2302). The TM-PLAT dominant negative phenotype is equivalent to the response and Lov defects of the *lov-1(sy582)* null mutant. The figure was generated using Sigmaplot5 (SPSS, Chicago, IL). Data are represented as mean  $\pm$  SEM. Single asterisk,  $p < 0.05$  compared with control. Double asterisk,  $p < 0.01$  compared with control.

expression of *atp-2* or RNA interference (RNAi) to ATP synthase components resulted in a specific defect in the response step of male mating behavior. These results sug-

gest that the unexpected localization of the ATP synthase to cilia plays a critical role in polycystin signaling, ciliary function, and sensory behaviors.

## MATERIALS AND METHODS

### Strains and Alleles

Nematode culturing and genetics were performed as described previously (Brenner, 1974). *him-5(e1490)* was used as the wild-type (Hodgkin, 1983). Several *C. elegans* strains were obtained from the *Caenorhabditis* Genetics Center. We constructed transgenic lines by injecting plasmid DNA (100–200 ng/ $\mu$ l) by using standard protocols (Mello and Fire, 1995). In all experiments, we used plasmid pBX containing the wild-type *pha-1(+)* gene as a cotransformation marker in the *pha-1(ts)* strain (Granato *et al.*, 1994).

### Molecular Biology Techniques

Details of plasmid constructions are available upon request. Standard procedures were used for recombinant DNA manipulations.

### Yeast Two-Hybrid

The yeast strain AH 109 (BD Biosciences Clontech, Palo Alto, CA) was used for Y2H experiments. Bait proteins were expressed in the GAL4 DNA-binding domain (DNA-BD) vector pGBKT7. A cDNA library derived from mix-staged *him-5* animals was constructed in the GAL4 activation domain (DNA-AD) vector pGAD GH. The PLAT domain of *C. elegans* LOV-1 (amino acids 2112–2302) and human PC-1 (amino acids 3164–3349) were used as baits in Y2H hybrids. Protein–protein interactions were accessed by growth rate on SD-Leu-Trp-His-Ade high-stringency plates and  $\beta$ -galactosidase filter assays. Both the *C. elegans* and human PLAT domain weakly interact with ATP-2 as judged by growth on SD-Leu-Trp-His-Ade. The interaction between the *C. elegans* and human PLAT domains is stronger with the amino terminus of ATP-1 (amino acids 1–209) as judged by growth on SD-Leu-Trp-His-Ade.

### In Vitro Binding

In vitro-translated Y2H candidate ATP-2 protein was produced with the TNT-quick coupled transcription/translation system (Promega, Madison, WI) by using [<sup>35</sup>S]methionine (Amersham Biosciences, Piscataway, NJ). A glutathione S-transferase (GST)-fused LOV-1 PLAT domain was produced in the bacterial strain BL21(DE3) and incubated with in vitro-translated candidates proteins in 500  $\mu$ l of binding buffer (20 mM Tris/Cl, pH 7.5, 150 mM NaCl, 5 mM MgCl<sub>2</sub>, 2 mM dithiothreitol, 0.05% NP-40) at 4°C for 30 min. Then, 25  $\mu$ l of glutathione-Sepharose 4B was added to the reaction and incubated at 4°C for an additional 2 h or overnight. After three washes with binding buffer, bound proteins were resuspended in 50  $\mu$ l of 1 $\times$  Laemmli buffer and then 10- $\mu$ l samples were boiled and separated by 10% SDS-PAGE. Proteins were visualized by Coomassie staining. The dried gel was exposed for autoradiography.

### Expression Analysis

Epifluorescence microscopy experiments were carried out by using a Zeiss Axioplan2 imaging system and photographed with an Orca-ER camera. Confocal experiments were carried out on a Bio-Rad MRC-1024 laser scanning confocal microscope.

### Rescue of *atp-2(ua2)* Mutant

LB128 *atp-2(ua2) unc-32(e189)/qC1 (ápy-19(e1259) glp-1(q339)* hermaphrodites were crossed by *him-5; myEx (ATP-2::GFP)* males. F2 progeny segregating Unc and green fluorescent protein (GFP)<sup>+</sup> were picked and maintained. Rescue of the L3 larval arrest in these lines was scored. All Unc GFP<sup>+</sup> animals were rescued for *atp-2(ua2)* L3 larval arrest.

### RNA Interference Assay and Mating Behaviors

For heat shock-inducible RNAi mediated by the inverted repeat (IR) genes (HS-IR-RNAi), we constructed IR genes as described previously (Tavernarakis *et al.*, 2000). Transgenic lines carrying IR plasmids were generated. Mix-staged transgenic animals were heat shocked for 4 h at 35°C, before returning to 15°C. After 63–67 h at 15°C, L4 males were transferred to new plates for culturing another 14 h at 15°C. Mating behaviors were scored as described previously (Barr and Sternberg, 1999). For tissue-specific RNAi (TS-IR-RNAi), we constructed IRs whose transcription is under the control of the *pkd-2* promoter. Transgenic lines were generated and males were scored for mating behaviors. For feeding RNAi, RNAi bacteria clones were obtained from MRC Geneservice (Cambridge, United Kingdom). Double-stranded RNA producing bacteria were grown in LB with 50 ng/ml ampicillin overnight at 37°C and seeded onto NGM agar plates, including additives (1 mM isopropyl  $\beta$ -D-thiogalactoside, 50 ng/ml ampicillin). The next day, 6–8 L4 stage RNAi-sensitive *rrf-3; him-5* hermaphrodites (Simmer *et al.*, 2002) were transferred onto feeding plates and incubated ~72 h at 15°C. L4 males were picked to new feeding plates seeded with feeding RNAi bacteria, cultured 14 h at 15°C, and the mating behaviors of adult males was scored. In all experiments, at least 24 animals were scored per experimental trial. Triplicate trials were performed for each line to obtain statistical data. All behavioral assays were done with the experimenter completely blinded to the sample.

## RESULTS

### Overexpression of the LOV-1 PLAT Domain Interferes with the Response and Vulva Location Male Mating Behaviors

*C. elegans* male mating behavior is a powerful in vivo assay for LOV-1 and PKD-2 polycystin function. The *C. elegans* male uses a series of both chemosensory and mechanosensory behaviors during mating. Male mating is the most complex behavior executed by *C. elegans*. The male nervous system possesses 381 neurons to the hermaphrodite's 302 (Sulston *et al.*, 1980; White *et al.*, 1986). Sexual dimorphism is reflected in behavior. Many of the 87 male-specific neurons mediate male mating behaviors (Figure 1a) (Liu and Sternberg, 1995). Male copulation is comprised of a stereotyped subseries of behaviors: response to hermaphrodite contact, backing along the hermaphrodite body, turning at the head or tail of the hermaphrodite, vulva location, spicule insertion, and sperm transfer. *lov-1* and *pkd-2* mutants are response and Lov (location of vulva) defective. Wild-type males have ~95% response and vulva location efficiency, whereas *lov-1* and *pkd-2* mutants exhibit ~25% response and vulva location efficiency (Figure 1b) (Barr and Sternberg, 1999; Barr *et al.*, 2001).

To ascertain the function of the PLAT domain, GFP-tagged PLAT domain transgenes were introduced into wild-type animals. The mating behavior of transgenic animals is scored, with response and Lov defects being an effective readout of interference with polycystin signaling. The strong *pkd-2* promoter is expressed in male-specific neurons of the head (the four CEMs) and tail (the B type neurons of rays and hook) (Figure 1a) (Barr and Sternberg, 1999; Barr *et al.*, 2001). The *pkd-2* promoter was used to drive expression of either the LOV-1 PLAT domain alone (PLAT) or a LOV-1 transmembrane segment followed by the PLAT domain (TM-PLAT) in wild-type animals. Overexpression of either PLAT or TM-PLAT interfered with response step of male mating behavior (Figure 1b). In contrast, only the TM-PLAT construct blocked both response and vulva location behaviors (Figure 1b), suggesting that PLAT-localization to the membrane is a requisite for vulva location behavior. The severity of response and Lov defects of the TM-PLAT dominant negative construct is identical to that of the *lov-1* mutant (Figure 1b). The dominant negative phenotypic differences between TM-PLAT and PLAT alone may reflect differential membrane targeting ability or effector interactions. With respect to the latter possibility, TM-PLAT may bind and inhibit the function of proteins required for both vulva location and response behaviors, whereas PLAT alone may bind and inhibit the function of proteins required for response behavior.

The PLAT domain has been proposed to mediate protein–protein or protein–lipid interactions (Bateman and Sandford, 1999). An alternative possibility is that the polycystin PLAT domain functions as a ciliary localization signal. LOV-1 and PKD-2 localize to the ciliated sensory endings of male-specific neurons (Figure 1a) (Barr and Sternberg, 1999; Barr *et al.*, 2001) and mammalian PC-1 and PC-2 localize to primary cilia of renal epithelia (Pazour *et al.*, 2002; Yoder *et al.*, 2002). Ciliary trafficking mechanisms are not well understood in any organism (reviewed by Rosenbaum and Witman, 2002). *C. elegans* is a useful model system to study protein sorting, transport, and localization (Koushika and Nonet, 2000). To test the hypothesis that the PLAT domain is responsible for ciliary targeting, we examined the subcellular localization of PLAT::GFP and TM-PLAT::GFP in wild-type males. Neither PLAT::GFP nor TM-PLAT::GFP local-



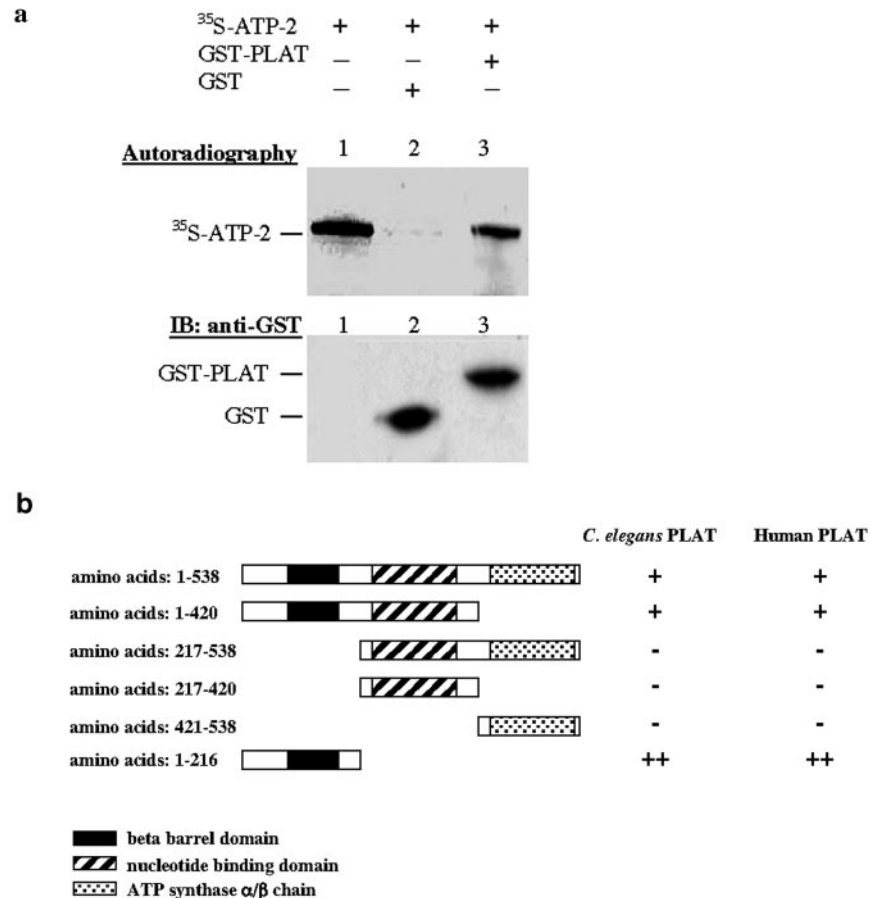


**Figure 2.** ATP-2 directly interacts with the LOV-1 PLAT domain. (a) GST pulldown assay showing the *in vitro* interaction between ATP-2 and the LOV-1 PLAT domain. *In vitro* translated <sup>35</sup>S-labeled ATP-2 protein was incubated with GST or GST-PLAT (amino acids 2112–2302). Autoradiography shows that the <sup>35</sup>S-labeled ATP-2 protein is specifically retained in the GST-PLAT column. A Western blot developed with anti-GST antibody shows the presence of GST and GST-PLAT in each column. (b) The ATP-2 N terminus is responsible for the interaction with the LOV-1 PLAT domain. Different *atp-2* truncation fragments were cloned into the Y2H pGADGH AD vector. *C. elegans* and human PLAT domain were engineered into the Y2H pGBKT BD vector. The Y2H interaction was accessed by the growth on selective media (SD-Leu-Trp-His-Ade, refer to *Materials and Methods*). ++, strong growth; +, weak growth; -, no growth.

izes to cilia, indicating that the PLAT domain is not sufficient for ciliary targeting (our unpublished data). Combined, these behavioral and cellular analyses suggest that the PLAT domain cannot localize to the normal site of LOV-1 action (the cilium) and may act by dominantly interfering with LOV-1 and/or its effectors.

#### ATP-2 Interacts with the PLAT Domain of LOV-1 and Human Polycystin-1

To test the hypothesis that the PLAT domain dominantly interferes with the function of LOV-1 effectors and to identify targets of the PLAT domain,  $1 \times 10^6$  cDNAs were screened for yeast two-hybrid interaction with the LOV-1 PLAT domain. Twenty plasmid-dependent interactors were isolated. The interactor ATP-2, an ATP synthase F<sub>1</sub> subunit, was isolated twice. The mitochondrial ATP synthase (also referred to as the mitochondrial respiratory chain [MRC] complex V) is a multimeric enzyme consisting of the soluble F<sub>1</sub> and membrane-bound F<sub>0</sub> complexes. *C. elegans* ATP-2 is the β subunit, or active site, of the F<sub>1</sub> portion (Tsang *et al.*, 2001). The MRC generates the majority of cellular ATP.

To demonstrate direct interaction between ATP-2 and LOV-1, a GST-PLAT fusion was expressed and purified from *Escherichia coli*. ATP-2 was *in vitro* transcribed and translated in the presence of radiolabeled [<sup>35</sup>S]methionine and then incubated with GST-PLAT, or GST as control, and glutathione-Sepharose 4B. Proteins were electrophoresed on SDS-PAGE, and gels were dried and exposed to film. [<sup>35</sup>S]ATP-2 binds to GST-PLAT but not GST alone, indicat-

ing that ATP-2 binds directly to the PLAT domain of LOV-1 (Figure 2a).

To determine whether the interaction between the PLAT domain and ATP-2 is evolutionarily conserved, we examined the association of the human PC-1 PLAT domain and *C. elegans* ATP-2. We find that ATP-2 also interacts with human PC-1 in a yeast two-hybrid assay (Figure 2b). We mapped the region of ATP-2 region responsible for the interaction with the PLAT domain of both human PC-1 and *C. elegans* LOV-1. The amino terminus of ATP-2 (amino acids 1–216), which contains a conserved β barrel domain, is the minimal PLAT binding region (Figure 2b). The β barrel domains of the α- and β-subunits are important for the assembly of the ATP synthase (Bakhtiari *et al.*, 1999). When compared with the full-length ATP-2 protein, the β barrel-containing ATP-2 fragment interacts more strongly with the PLAT domains of both PC-1 and LOV-1 (Figure 2b). That ATP-2 associates with the PLAT domains of both PC-1 and LOV-1 PLAT domain supports our hypothesis that there exists an intracellular polycystin signaling pathway conserved throughout evolution.

#### *atp-2* Is Coexpressed with *lov-1*

Next, we examined the expression pattern of *atp-2* by using a 1.5-kb *atp-2* promoter fragment to drive GFP expression. *Patp-2::GFP* (P for promoter) is widely expressed throughout development in both males and hermaphrodites (our unpublished data). Consistent with the broad spatial and temporal expression, the nuclear-en-

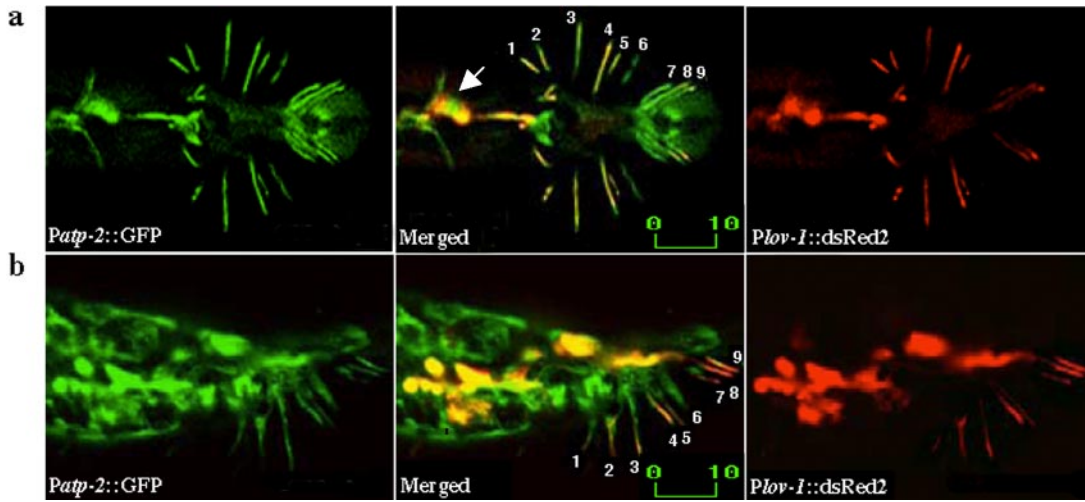


**Figure 3.** *atp-2* is coexpressed with *lov-1* in RnB and HOB neurons. (a and b) Confocal micrographs of *Patp-2::GFP* and *Plov-1::DsRed2* double-labeled males. Ventral up view (a) or side view (b) of the *C. elegans* adult male tail. Note the presence of *Patp-2::GFP* in all nine pairs of RnB neurons and the exclusion of *Plov-1::DsRed2* in Ray 6 neuron. Numbers indicate the dendrites of corresponding rays. The arrow points to the location of the HOB neuron. Labeled bar indicates length in micrometers.

coded *atp-2* gene is required for embryonic and larval development (Gonczy *et al.*, 2000; Tsang and Lemire, 2002). To determine whether *atp-2* and *lov-1* are coexpressed, the male-specific neurons of the head and tail were double labeled with *Patp-2::GFP* and *Plov-1::DsRed2* (a 3-kb *lov-1* promoter driving expression of *Discosoma* red fluorescent protein). *lov-1* and *atp-2* are coexpressed in the tail ray B neurons and HOB hook neuron (Figures 3 and 5a) as well as the male-specific CEM head neurons.

**ATP-2 and Other ATP Synthase Components Localize to Ray and CEM Cilia**

ATP-2 is predicted to localize to the inner mitochondrial membrane with the MRC. In contrast, LOV-1 and PKD-2 proteins localize to cilia and intracellular membranes (Barr and Sternberg, 1999; Barr *et al.*, 2001). PKD-2 and LOV-1 do not possess mitochondrial transport signals and do not localize to mitochondria (Figure 4c, c'). Furthermore, cilia do not contain mitochondria (Figure 4b, dashed box; note that

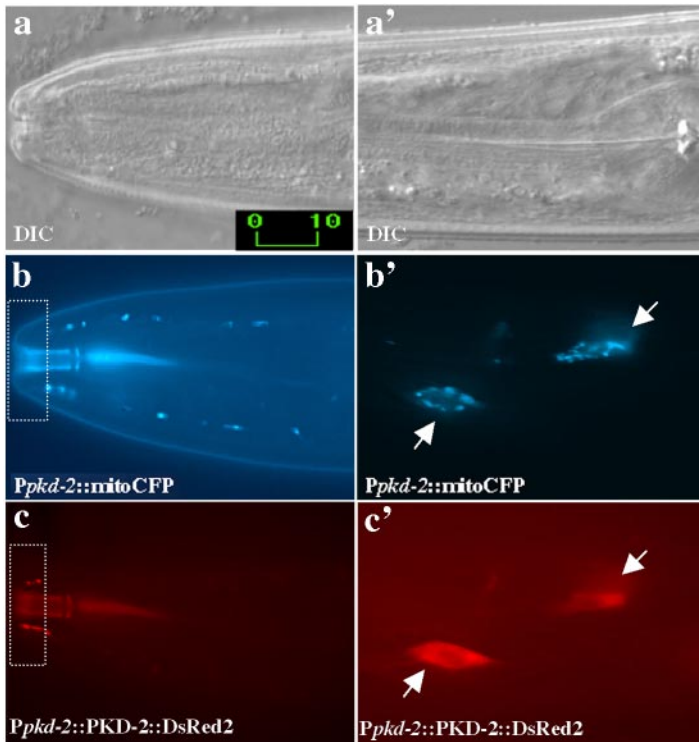


**Figure 4.** PKD-2 does not localize to mitochondria and mitochondria are not found in cilia. (a and a') Differential interference contrast images of the *C. elegans* adult male nose (a) and pharyngeal (a') regions of the head. Corresponding epifluorescence images of cyan fluorescent protein (CFP) with mitochondrial localization signal (mitoCFP) (b and b') and PKD-2::DsRed2 in CEM neurons (c and c'). Mitochondria exhibit a dot-spot like pattern in the cell body (b'), dendrite (b'), but not in cilium (b). PKD-2::DsRed2 localizes to cilia (c) and intracellular membranes (c') of the CEMs. Arrows point to the CEM neuronal cell bodies. Dashed rectangular boxes show the ciliary zone of CEM neurons. Labeled bars indicate length in micrometers.

in all figures, dashed boxes indicate ciliary regions of sensory neurons.) We observe the absence of mitochondria from cilia by using both fluorescence and electron microscopy. A mitochondrial targeted, cyan-shifted GFP (*Ppkd-2::mitoCFP*) is present in neuronal axons, cell bodies, and dendrites (Figure 4b, b') but is obviously excluded from cilia (Figure 4b). Electron micrographs of male sensory rays show that mitochondria are present only within the dendritic portion of the neuron processes but not within the cilium (David Hall, personal communication). Therefore, the interaction between the mitochondrial ATP-2 and ciliary LOV-1 protein is unexpected and surprising.

To determine whether ATP-2 and LOV-1 colocalize in the cell, subcellular localization of ATP-2 was examined. A 1.5-kb native *atp-2* promoter was used to drive expression of the *atp-2* cDNA fused to GFP (*Patp-2::ATP-2::GFP*). To first demonstrate that ATP-2::GFP is functional and expression/localization patterns are physiologically relevant, we introduced the *Patp-2::ATP-2::GFP* construct into the *atp-2(uo2)* deletion strain. *Patp-2::ATP-2::GFP* completely rescues the L3 arrest and embryo lethality phenotype of the *atp-2(uo2)* deletion strain (our unpublished data). ATP-2::GFP is found in a broad range of tissue types (Figure 5, a and b, left), making it difficult to ascertain ciliary localization. To look more carefully at ATP-2 subcellular localization, we examined colocalization of ATP-2 and PKD-2. LOV-1 and PKD-2 exhibit identical subcellular localization patterns (Barr and Sternberg, 1999; Barr *et al.*, 2001). PKD-2 is expressed at much higher levels than LOV-1, making PKD-2 more useful for microscopic analysis (our unpublished data). PKD-2::DsRed2 localizes to cilia and cell bodies of ray, HOB (Figure 5a, right), and CEM neurons (Figure 5b, right). ATP-2::GFP clearly colocalizes with PKD-2::DsRed2 in CEM cilia (Figure 5b, middle). In rays and HOB, ciliary colocalization of ATP-2 and PKD-2 was ambiguous due to the expression of ATP-2::GFP in ray neurons, support cells, and hypodermis.

To specifically determine the subcellular localization of ATP-2 in male sensory neurons, the *pkd-2* promoter was used to drive expression of ATP-2::GFP in the CEMs, rays, and HOB neurons (*Ppkd-2::ATP-2::GFP*; Figure 5, c–e). Using this cell-specific construct, ATP-2 clearly localizes to cilia in ray (Figure 5c, dashed box), CEM (Figure 5, d and e, dashed box), and HOB neurons. As expected, ATP-2::GFP also is observed in mitochondrial-like structures within dendrites, cell body, and axons (compare *Ppkd-2::ATP-2::GFP* in Figure 5d with *Ppkd-2::mitoCFP* in Figure 4b, b'), consistent with conventional mitochondrial localization.

ATP-2 is one subunit of the ATP synthase. The ATP synthase is composed of a membrane-bound proton channel ( $F_0$ ) and a peripheral catalytic complex ( $F_1$ ). We reasoned that other subunits of the ATP synthase may be present with ATP-2 in cilia. ASB-1 is a subunit of the  $F_1$  complex and ASG-2 is a membrane protein component of the  $F_0$  proton channel. We find that GFP-tagged ASB-1 and ASG-2 localize to male-specific sensory cilia as well as mitochondria (Figure 6, left and middle). The MRC is composed of four electron transporting complexes (I–IV) and the ATP synthase (complex V). NUO-1 (NADH/ubiquinone oxidoreductase) is a complex I component. In contrast to the ATP synthase, NUO-1::GFP is not found in the ciliary compartment (Figure 6, right). Thus, these distinct subcellular localizations point at an additional and nonmitochondrial related function for the ATP synthase in cilia of male-specific sensory neurons.

#### *atp-2* and MRC Complex V Are Required for Male Response Behavior

We next asked whether *atp-2* and other ATP synthase components are required for *lov-1*-mediated response and vulva location behaviors. *atp-2* is an essential gene (Gonczy *et al.*, 2000; Tsang *et al.*, 2001). *atp-2(uo2)* mutants arrest at the third larval stage (L3), and both *atp-2(uo2)* and *atp-2* RNAi result

**Table 1.** RNAi to MRC Complex V but not Complex I, II, or III interferes with response

| Gene (MRC Complex)       | Gene name, predicted protein product | Published RNAi phenotype | F1 feeding phenotype | F2 feeding phenotype | F1 mating behavior |          | F2 mating behavior |          |
|--------------------------|--------------------------------------|--------------------------|----------------------|----------------------|--------------------|----------|--------------------|----------|
|                          |                                      |                          |                      |                      | Response           | LOV      | Response           | LOV      |
| C09H10.3 (Complex I)     | <i>mdo-1</i> , NADH Dehydrogenase    | Emb, Lva                 | Emb, Gro, Sma        | Emb, Gro, Ste        | 81.6±3.5           | 87.5±3.1 | 75                 | 88.1     |
| F42A8.2 (Complex II)     | Succinate dehydrogenase Fe-S         | Bmd, Clr, Emb, Gro, Lva  | Emb, Gro             | Emb, Gro, Lva        | 88.3±3.1           | 86.8±1.3 | 86.2               | 87.5     |
| ZC116.2 (Complex III)    | Cytochrome C                         | WT                       | Gro, Sma             | Emb, Gro, Sma        | 87.5±7.2           | 88.7±2.7 | 78.6               | 90.5     |
| F35G12.10 (Complex V/F0) | <i>asb-1</i> , subunit B             | Emb, Gro, Ste, Stp       | Emb, Gro             | Emb, Gro, Ste        | 67.3±6.9           | 92.5±0.9 | 66.7               | 90       |
| F02E8.1 (Complex V/F0)   | <i>asb-2</i> , subunit B             | Lva                      | Minor Gro            | Minor Gro            | 86.1±6.4           | 90.3±2.9 | 83.3               | 90       |
| C53B7.4 (Complex V/F0)   | <i>asg-1</i> , subunit G1            | Bmd, Emb, Etv, Gro, Stp  | Emb, Gro             | Gro, Emb             | 83.3±4.2           | 90.7±4.6 | 87.5               | 91.3     |
| K07A12.3 (Complex V/F0)  | <i>asg-2</i> , subunit G2            | Gro, Clr                 | Emb, Gro             | Emb, Gro, Ste        | 86.1±4.9           | 94.4±3.0 | 54.3±3.5           | 87.1±1.6 |
| F58F12.1 (Complex V/F1)  | Delta chain                          | Emb, Gro, Lva            | Minor Gro            | Minor Gro            | 90.3±2.4           | 93.0±2.2 | 83.3               | 91.3     |
| R05D3.6 (Complex V/F1)   | Epsilon chain                        | WT                       | Minor Gro            | WT                   | 94.5±4.8           | 92.5±3.6 | 87.5               | 93.8     |
| C34E10.6 (Complex V/F1)  | <i>atp-2</i> , Beta chain            | Emb, Lva, Ste            | Emb, Gro, Lva, Ste   | N/A                  | 34.7±21.2          | 92.5±4.5 | N/A                | N/A      |

RNAi knock-down components from MRC complex V but not Complex I, II, or III affects the response, but not vulva location, step of mating behavior. RNAi and mating behavior assays were performed as described in *Materials and Methods*. Bacterial strains of feeding RNAi clones were obtained from MRC Geneservice (United Kingdom). In all experiments, at least 24 animals were scored blindly per experimental trial. Triplicate trials were performed for each line to obtain statistical data. Column 1 lists the gene by cosmid number; the MRC complex with which it is associated is indicated in parentheses. Column 2 indicates three-lettered italicized gene name and/or predicted protein product. Column 3 lists published RNAi phenotypes (Fraser *et al.*, 2000; Gonczy *et al.*, 2000b; Hanazawa *et al.*, 2001; Kamath *et al.*, 2003; Piano *et al.*, 2002; Simmer *et al.*, 2003). Phenotypic abbreviations: Bmd, body morphology defect; Clr, clear; Emb, embryonic lethal; Etv, embryonic terminal arrest variable; Gro, slow growth; Lva, larval lethal; Sma, small; Ste, sterile; Stp, sterile progeny; WT, wild type. Columns 4 and 5 describe RNAi phenotypes of F1 and F2 progeny observed in this study. The remaining columns provide quantitative RNAi feeding data for F1 and F2 male response and vulva location (LOV) behaviors in mean ± S.E.M. RNAi of genes resulting in a response defective phenotype are circled. N/A indicates not applicable as F1 progeny were sterile and unable to produce F2 offspring.



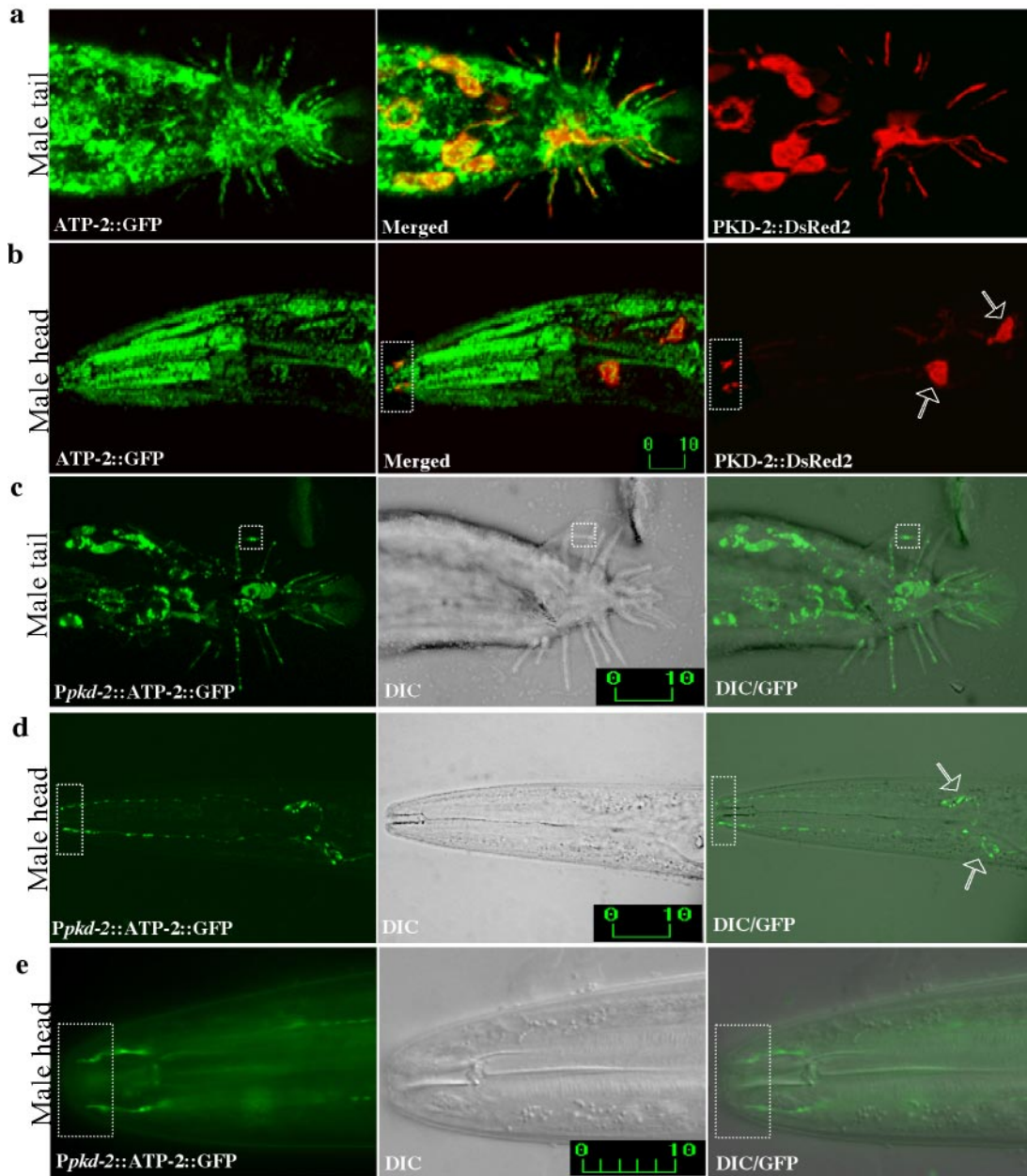


**Figure 5.** ATP-2 localizes to both cilia and mitochondria of male-specific neurons. (a and b) Confocal micrographs of *Patp-2::ATP-2::GFP* (left) and *Ppkd-2::PKD-2::DsRed2* (right) double-labeled males (merge in middle). Adult male tail (a) and adult male head (b). PKD-2 and ATP-2 localize to cilia in the male-specific neurons RnBs, HOB, and CEMs. (c–e) Confocal epifluorescence micrographs (left), differential interference contrast (DIC) (middle), and epifluorescence/DIC images (right) of males expressing *Ppkd-2::ATP-2::GFP*. ATP-2 expression was restricted to male-specific neurons by using a 1.3-kb *pkd-2* promoter. (c) ATP-2 localizes to ray cilia (dashed box) and mitochondria. (d and e) ATP-2 localizes to both mitochondria and cilia of CEMs. Hollowed arrows indicate CEM neuronal cell bodies. (e) Higher magnification of the nose region showing ciliary localization of ATP-2. Dashed rectangular boxes show the ciliary zone of the CEM neurons. Labeled bars indicate length in micrometers.

in behavioral defects, including impaired locomotion, pharyngeal pumping, defecation, and dauer formation (Gonczy *et al.*, 2000). To circumvent earlier developmental requirements and analyze the role of *atp-2* in the adult male, we lowered the activity of *atp-2* with RNAi. We used two RNAi methods: feeding animals with bacteria producing double-stranded RNA (dsRNA) (Timmons *et al.*, 2001) and *in vivo* production of dsRNA from transgenic promoters (Tavernarakis *et al.*, 2000). *C. elegans* neurons are largely resilient to the effects of RNAi for elusive reasons (Tavernarakis *et al.*,

2000; Kamath *et al.*, 2001; Timmons *et al.*, 2001). In our hands, RNAi feeding is successful with *rrf-3(pk1429)* animals that are RNAi hypersensitive. IR plasmids producing dsRNA are also effectual at knocking down gene function in neurons. The latter is particularly valuable for temporal or tissue-specific gene knockdown by using appropriate promoters.

Feeding RNAi of *atp-2* resulted in sterility (Ste), embryonic lethality (Emb), and larval arrest (Lva) (Table 1). Those males that survived to adulthood were response defective with intact vulva location behavior (Table 1 and Figure 7c).

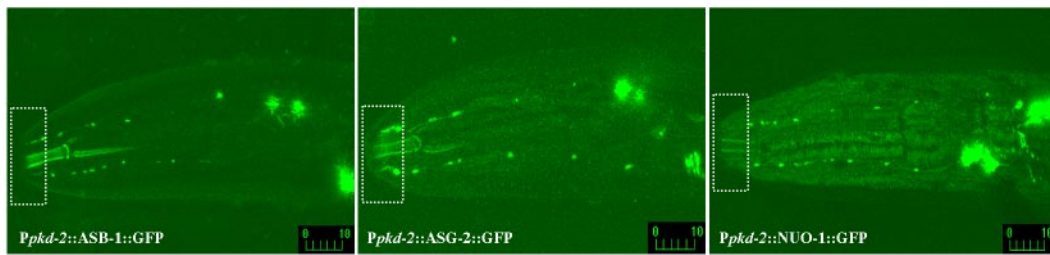


**Figure 6.** ATP synthase components ASG-2 and ASB-1 localize to CEM cilia. Confocal micrographs of *Ppkd-2::ASG-2::GFP*– (left) and *Ppkd-2::ASB-1::GFP*– (middle)–labeled males. ASG-2 and ASB-1 expression was restricted to male-specific neurons by using a 1.3-kb *pkd-2* promoter. ASG-2 and ASB-1 localize to both mitochondria and cilia of CEMs. Another mitochondria protein that is not a component of the ATP synthase, NUO-1::GFP, did not localize to cilia. Dashed rectangular boxes show the ciliary zone of the CEM neurons. Labeled bars indicate length in micrometers.

A response defect also was observed with *atp-2* IR plasmids producing dsRNA. We used either the HS-IR-RNAi or *pkd-2* promoter (TS-IR-RNAi) to drive expression of *atp-2* cDNA IRs. Knockdown of *atp-2* function by either HS-IR-RNAi or TS-IR-RNAi consistently resulted in response but not vulva location defects (Figure 7a, b). We also found that multicopy expression of *atp-2*, *atp-2(xs)* for excess, by using *Patp-2::ATP-2::GFP* (Figure 7d) or *Ppkd-2::ATP-2::GFP* (Figure 7e), interfered with response but not vulva location behavior. These results indicate that *atp-2* is required in cell autonomous manner for response behavior and that *atp-2* function may be required in the cilia of ray but not hook neurons.

An alternative possibility is that the response defect results simply from disrupting mitochondrial activity in neurons. To distinguish between mitochondrial and ciliary function, we knocked down the activity of components in the electron transport chain and the ATP synthase. Feeding RNAi of genes encoding complex I, II, III, and V produced phenotypes associated with loss of mitochondrial function (Emb, Lva, and slow growth, Gro; Table 1). However, RNAi of only components in complex V, the ATP synthase, but not other respiratory chain components affected response behavior (Figure 7c and Table 1). RNAi feeding of *atp-2*, *asb-1*, and *asg-2* reduced male response behavior from 90 to 35, 67, and 54%, respectively (Table 1). Tissue-specific RNAi of *asb-1*, *asg-2*, and *atp-2* produced similar response defects (Figure 7B), whereas tissue-specific RNAi of a complex III component, ZC116.2 cytochrome C, did not (our unpublished data). We observed that RNAi treatment of some predicted components in ATP synthase caused no response defects (Table 1). Perhaps the ciliary ATP synthase has a different subunit composition than the mitochondrial ATP synthase or these genes are simply not sensitive to feeding RNAi treatment. Regardless, these results indicate that the ATP synthase components ATP-2, ASB-1, and ASB-2 are specifically required in cilia of male ray neurons for response behavior.

One concern is that neurons depleted of *atp-2* become generally unhealthy. We observe no neurodegeneration in male sensory neurons with HS-IR-RNAi, TS-IR-RNAi, or *atp-2(xs)* (our unpublished data). CEM cilia also form normally in animals overexpressing *atp-2*, *asb-1*, and *asg-2* (Figures 5e and 6). We conclude that the ATP synthase is required for the function but not development of ciliated male sensory neurons.

#### **ATP-2 Does Not Localize to AWA Cilia and Is Not Required for Olfactory Behaviors**

Does the ATP-2 synthase function in all ciliated sensory neurons? Sensory cilia are found in 60 of the 302 neurons in

the *C. elegans* hermaphrodite and in 112 of the 381 neurons in the male (Sulston *et al.*, 1980; White *et al.*, 1986). To test the involvement of *atp-2* in other ciliated neurons, we examined ATP-2 localization and function in the amphid AWA sensory neuron pair. The AWA olfactory neurons sense attractive odorants, including diacetyl (Bargmann *et al.*, 1993). The G protein-coupled odorant receptor ODR-10 is expressed and required in the complex, fork-shaped cilia of AWA neurons (Sengupta *et al.*, 1996). To determine whether ATP-2 localizes to AWA cilia, we used the *odr-10* promoter to drive the expression of ATP-2::GFP (Figure 8a) or ODR-10::GFP (Figure 8b). In AWA neurons, ATP-2::GFP is exclusively found in mitochondria and does not localize to cilia (Figure 8a). Two conclusions may be drawn from this result. First, the ciliary localization of ATP-2 in male-specific neurons reflects endogenous localization and is not an artifact of GFP overexpression. Second, the ciliary localization of ATP-2 is restricted to subset of sensory neurons.

To confirm that ATP-2 does not function in AWA olfactory neurons, we examined the effects of *atp-2* tissue-specific RNAi and overexpression in the AWA olfactory neurons by using the *odr-10* promoter. When the AWA neurons are killed with a laser microbeam, animals are unable to chemotax to diacetyl (Bargmann *et al.*, 1993). Likewise, animals with abnormal AWA cilia, such as *osm-5* mutants, exhibit diacetyl chemotaxis defects (Figure 8c) (Bargmann *et al.*, 1993). Neither knockdown nor overexpression of *atp-2* affected AWA-mediated diacetyl chemotactic behaviors (Figure 8c). These findings show that reducing activity of *atp-2* or overexpression of *atp-2* does not result in nonspecific disruption of sensory neuron function. We conclude that the ATP synthase is specifically required in ray cilia for response behavior.

#### ***atp-2* and *lov-1* Act in the Same Molecular Pathway**

Two simple models could explain the response-defective phenotype. In the first, the ATP synthase and polycystins act in the same molecular pathway. Alternatively, the ATP synthase and polycystins function in parallel pathways mediating response behavior. To distinguish between these possibilities, we examined the effects of *atp-2* RNAi in *lov-1* and *pkd-2* null mutant backgrounds. We reasoned that if *atp-2*, *lov-1*, and *pkd-2* act in different pathways, we would observe an additive effect and a more severe response defect than loss of either alone. We find that the response defect of *lov-1(sy552)* and *pkd-2(sy606)* mutants is not increased further by treatment with *atp-2* RNAi (our unpublished data). These results show that *atp-2*, *lov-1*, and *pkd-2* act in the same pathway regulating response behavior.



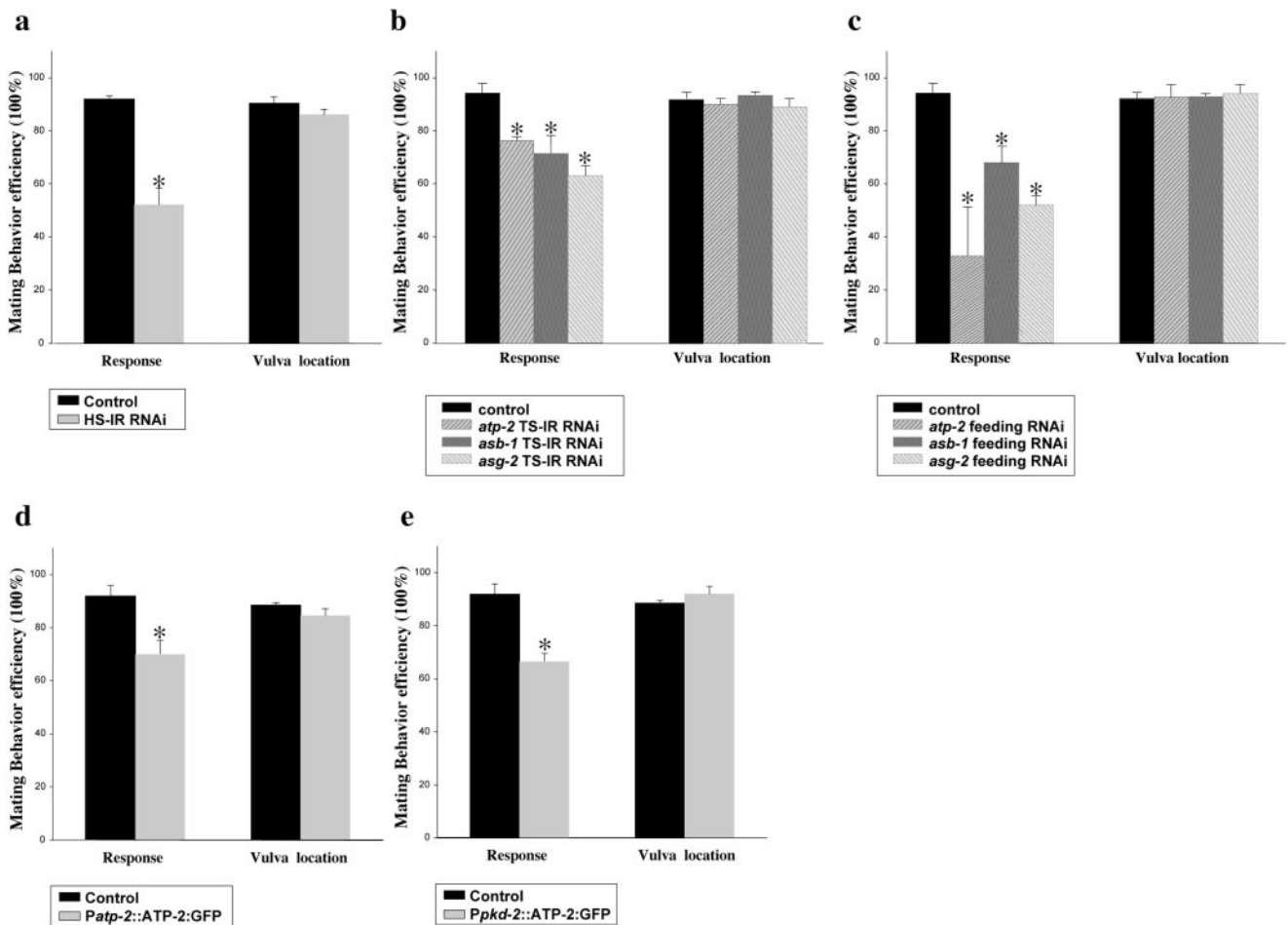


**Figure 7.** *atp-2* and MRC complex V are required for response behavior. (a–c), Knocking down *atp-2* and MRC complex V components in wild-type *C. elegans* males by RNAi affects the response step of mating behavior, but not vulva location. RNAi and mating behavior were performed as described in *Materials and Methods*. (a) HS-IR RNAi, 1.3-kb inverted-repeat *atp-2* cDNA was cloned into pPD49.78 heatshock vector. (b) TS-IR RNAi IR fragments of the *atp-2*, *asb-1*, and *asg-2* cDNAs were cloned downstream of 1.3-kb *pkd-2* promoter. (c) Feeding RNAi, bacterial strains of the *atp-2* feeding RNAi clone (III-2B16), *asb-1* (III-2E22), and *asg-2* (I-4E04) were obtained from MRC geneservice (Cambridge, United Kingdom). (d and e) Overexpression of *atp-2* in wild-type males leads to a defect in the response, but not vulva location, step of mating behavior. (d) A 1.5-kb *atp-2* promoter was used to drive the broad expression of *atp-2* cDNA. (e) A 1.3-kb *pkd-2* promoter was used to drive the expression of *atp-2* cDNA in only male-specific neurons. In all experiments, at least 24 animals were blindly scored per trial. For each line, experiment trials were done in triplicate trials to obtain statistical data. Figures were generated using Sigmaplot5 (SPSS). Data are represented as mean  $\pm$  SEM. Asterisk,  $p < 0.05$  compared with control.

What is the significance of the LOV-1 and ATP-2 binding? LOV-1 may be required for ATP-2 localization to cilia or vice versa. We examined *Ppkd-2::ATP-2::GFP* localization in the *lov-1* mutant. ATP-2::GFP ciliary localization is identical in wild-type and *lov-1* mutants (our unpublished data). We conclude that *lov-1* is not required for ATP-2 localization in cilia. An interesting possibility is that ATP-2 localization changes under conditions of mating stimulation by hermaphrodite partners. However, we observe no gross differences in ciliary ATP-2::GFP localization or dendritic mitochondrial distribution in virgin L4 males and mated adult males nor in wild-type versus sensory defective *lov-1* mutants (our unpublished data).

Next, we compared PKD-2::GFP localization in wild-type and *atp-2* RNAi-treated animals. PKD-2::GFP ciliary localization is not obviously affected by *atp-2* TS-IR RNAi, although increases in dendritic PKD-2::GFP expression are observed (our unpublished data). These results indicate that ATP-2 is not essential for PKD-2 ciliary localiza-

tion. We hypothesize that a common mechanism may be required for the ciliary localization of ATP-2, LOV-1, and PKD-2.

## DISCUSSION

We have demonstrated that overexpression of the PLAT domain of LOV-1 dominantly interferes with polycystin function, perhaps by binding downstream effectors. We identify ATP-2 as a PLAT interactor in a yeast two-hybrid screen, show that this interaction is evolutionarily conserved, and biochemically demonstrate a direct interaction between ATP-2 and the LOV-1 PLAT domain. GFP-tagged ATP-2 colocalizes in vivo with the *C. elegans* polycystins. The unexpected ciliary colocalization of ATP-2 with LOV-1 and PKD-2 in male-specific sensory neurons suggests that ATP-2 may be involved in a polycystin signaling pathway. To test this hypothesis, various RNAi methods to knockdown *atp-2* were performed. Feeding RNAi, HS-IR-RNAi, and TS-IR

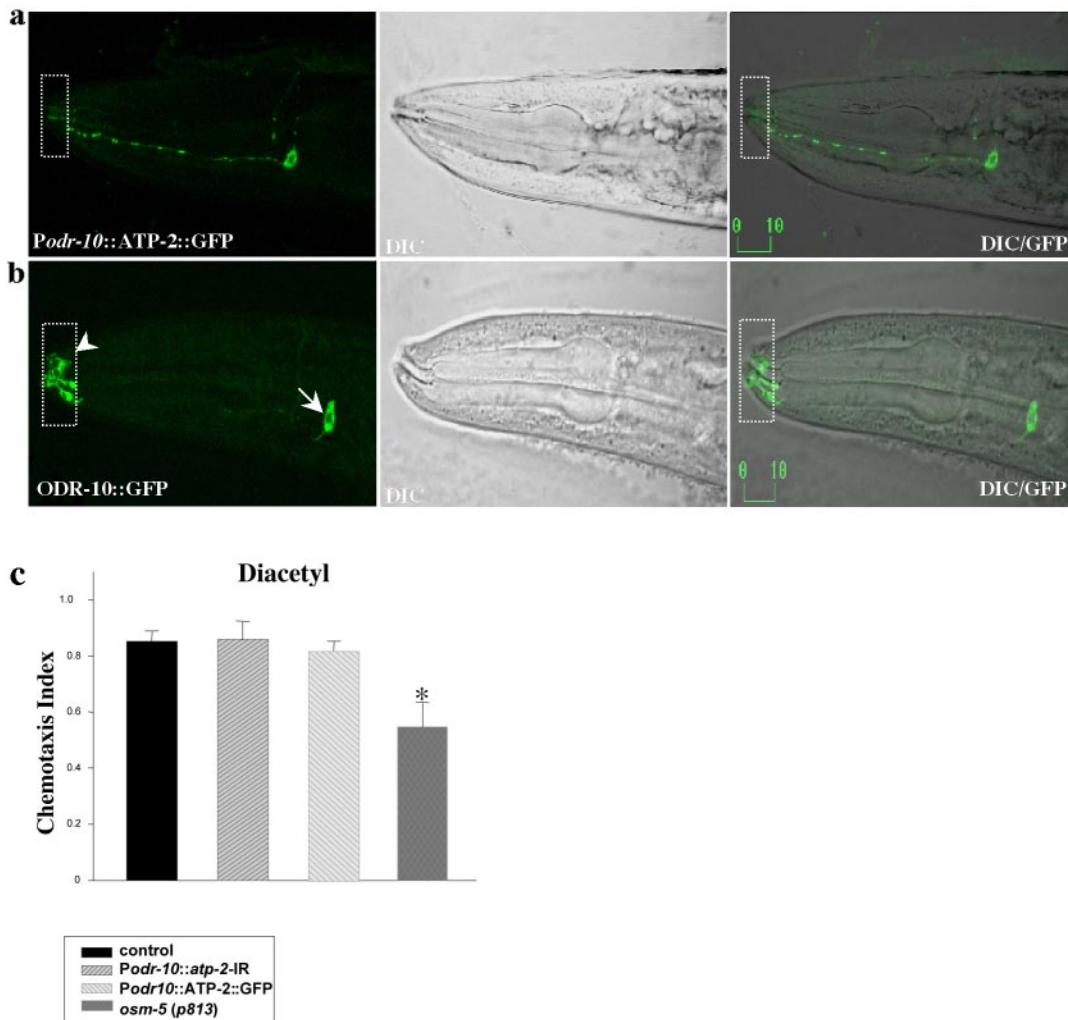


**Figure 8.** ATP-2 does not function or localize in the cilia of AWA sensory neurons. (a and b) Confocal micrographs of *Podr-10::ATP-2::GFP*–(a) and *Podr-10::ODR-10::GFP* (b)-labeled animals. A 1.0-kb *odr-10* promoter was used to drive expression of either ATP-2::GFP or ODR-10::GFP in olfactory AWA sensory neurons of the head. (a) ATP-2::GFP is restricted to mitochondria and absent from the cilium in an AWA neuron. Dashed rectangular boxes show the absence of ATP-2::GFP in the ciliary zone of the AWA neurons. (b) ODR-10::GFP protein is enriched in the cell bodies (arrow) and complex fork-shaped cilia (arrowhead) of AWA neurons. Labeled bars indicate length in micrometers. (c) TS-IR-RNAi of *atp-2* or overexpression of ATP-2::GFP does not affect AWA olfactory neuron function. Chemotaxis responses to the odorant diacetyl of the wild-type positive control, the negative control *osm-5(p813)*, and transgenic animals expressing *Podr-10::ATP-2::GFP* or *Podr-10::atp-2-IR* RNAi. Chemotaxis assays were performed as described in Sengupta *et al.* (1996). Diacetyl was diluted 1:1000 in ethanol. Chemotaxis index = (no. animals at the odorant vs. no. animals at the control)/total animals on plate. Approximately 200 animals were used in each assay. Four to six assays were performed for each group. Data are represented as mean  $\pm$  SEM. Asterick,  $p < 0.01$  compared with wild-type control, *Podr-10::ATP-2::GFP*, and *Podr-10::atp-2-IR* RNAi.

RNAi to *atp-2* as well as overexpression of *atp-2* all exhibited a similar phenotype: a defect in the response step of male mating behavior. *atp-2* RNAi does not exacerbate the response defects of *lov-1* and *pkd-2* mutants, indicating that ATP-2 and the *C. elegans* polycystins act in concert. Interestingly, *atp-2(xs)* has a dominant negative effect on response behavior, suggesting that overexpression of ATP-2 blocks the function of LOV-1 or the ATP synthase. Only MRC complex V, i.e., the ATP synthase, is required for response behavior. Consistent with this is the observation that two additional components of the ATP synthase, ASB-1 and ASG-2, localize to male specific sensory neuron cilia. Collectively, these results show that ATP-2 physically associates with the LOV-1 PLAT domain, localizes to cilia of male-specific sensory neurons, and acts in the polycystin signaling pathway regulating response behavior.

The ATP synthase is composed of two functional domains, a catalytic  $F_1$  portion and a membrane embedded  $F_0$  portion.  $F_1$  contains multiple subunits ( $\alpha_3\beta_3\gamma$ ,  $\delta$ ,  $\epsilon$ ) and is bound on the membrane by its interaction with  $F_0$ .  $F_0$  functions as a proton pump, and  $F_1$  uses the energy produced from proton translocation to synthesize ATP (Penefsky and Cross, 1991). The ATP synthase localizes primarily to inner mitochondria membrane (Boyer, 1997). However, the presence of ATP synthase at the cell membrane of lymphocytes, human endothelial cells, and hepatocytes has been reported (Das *et al.*, 1994; Moser *et al.*, 1999; Moser *et al.*, 2001; Chang *et al.*, 2002; Arakaki *et al.*, 2003; Martinez *et al.*, 2003). The polycystins also have been localized to lymphocytes, endothelial cells, and hepatocytes (Geng *et al.*, 1996; Ibraghimov-Beskrovnaya *et al.*, 1997; Aguiari *et al.*, 2004). ADPKD extrarenal manifestations include liver cysts and vascular

abnormalities (Igarashi and Somlo, 2002). In lymphocytes, membrane-bound ATP synthase was suggested to play a role in lymphocyte-induced tumor destruction (Das *et al.*, 1994). Endothelial cell membrane-bound ATP synthase was proven to be active in ATP synthesis and involved in angiogenesis (Moser *et al.*, 1999; Moser *et al.*, 2001) and endothelial cell proliferation (Chang *et al.*, 2002). This nonmitochondrial ATP synthase catalyzes ATP synthesis and is inhibited by angiostatin and an inhibitor of the F1 subunit (IF1), especially at low, tumor-like extracellular pH (Burwick *et al.*, 2004). Most recently, the ATP synthase has been found in plasma membrane lipid rafts along with  $\beta$ -tubulin (Bae *et al.*, 2004; Li *et al.*, 2004). Our results suggest that the ciliary localized ATP synthase may play a previously unsuspected role in polycystin signaling.

Whereas *lov-1* and *pkd-2* mutants are response and Lov defective, RNAi treatment of ATP synthase components or overexpression of *atp-2* causes only response but not Lov mating behavior defects. LOV-1 may have tissue-specific effectors. In other words, ATP-2 may be required for polycystin-mediated signaling in ray neurons (with defects resulting in abnormal male response behaviors) but not the HOB hook neuron (as evidenced by wild-type vulva location behavior). Given the diverse clinical manifestation of ADPKD and broad distribution of the polycystins, it is likely that the polycystins will have tissue-specific regulators and targets.

We propose two models for the role of the ATP-2 within cilia. In the first model, the ATP synthase may provide the source of energy for mitochondria-less cilia. Cilia require an energy source for ATP-dependent processes such as intraflagellar transport, which is required for the assembly and maintenance of all cilia and flagella (Rosenbaum and Witman, 2002). Defects in ciliary development or signaling may result in polycystic kidney disease (Watnick and Germino, 2003). In the second model, the ATP synthase may be involved in regulating intracellular or extracellular concentrations of ATP. ATP-2 may modulate intracellular ATP and ion homeostasis by regulating ion channel and/or transporter activity, with defects resulting in abnormal secretion or absorption, culminating in cystogenesis. In both models, the ATP synthase would require a proton gradient across the ciliary membrane to synthesize ATP. In this case, the ciliary membrane is predicted to contain  $\text{Na}^+/\text{H}^+$  exchangers and/or proton channels responsible for establishing the proton gradient.

The extracellular domain of LOV-1 possesses a predicted ATP/GTP binding site, or P loop, of unknown function (ASNIVGKT, amino acids 1691–1699). Extracellular ATP may bind to this site and modulate LOV-1 activity. Extracellular ATP has been shown to bind certain sites on the *N*-methyl-D-aspartate receptor and act as a positive allosteric modulator of channel gating (Kloda *et al.*, 2004). In mammalian cells, extracellular ATP regulates fluid secretion and cell volume via purinergic receptors (Leipziger, 2003). In fact, ATP release and signaling is increased in PKD cell culture systems (Schwiebert and Zsembery, 2003). ATP and the PC-1 C termini have been shown to regulate chloride secretion and cyst growth in ADPKD (Wilson *et al.*, 1999; Schwiebert *et al.*, 2002; Hooper *et al.*, 2003). Dysregulation of ATP synthase activity at the cell surface in ADPKD cysts may result in increases in ATP release and inappropriate chloride channel or purinergic receptor activation. Alternatively, ATP levels may regulate ATP-sensitive channels, including ATP-binding cassette transporters such as the cystic fibrosis transmembrane regulator chloride channel. Defec-

tive PC-1 calcium signaling has been implicated in ATP-stimulated chloride secretion (Wildman *et al.*, 2003).

This report is the first to assign function the polycystin-1 PLAT domain and to demonstrate ciliary localization of the ATP synthase. The cilium is an exclusive organelle in that it is not readily accessible to proteins, in particular membrane-bound proteins (Rosenbaum and Witman, 2002). How the ATP synthase localizes to the cilium is an intriguing mechanistic question. Although we have ruled out an essential role for LOV-1 in localizing ATP-2 to cilia (and vice versa), the function of the LOV-1 and ATP-2 interaction remains to be determined. Whether the ATP synthase and PC-1 colocalize in the primary cilium of renal epithelial cells is unknown. Our studies using *C. elegans* as a model for ADPKD promise new avenues to understanding polycystin function and ciliary sensory signaling.

## ACKNOWLEDGMENTS

We are grateful to Dr. David Hall for sharing unpublished electron micrograph data on ultrastructural anatomy of male sensory neurons, Drs. Gregory Germino and Feng Qian for the human PKD-1 cDNA, Douglas Braun for generating the male-enriched *C. elegans* yeast two-hybrid library, Dr. Karla Knobel for *pkd-2* promoter constructs and *lov-1* cDNAs, Dr. Juan Wang for advice on RNAi experiments, the *Caenorhabditis* Genetics Center for strains, Dr. Andrew Fire for providing *C. elegans* vectors, Dr. Cori Bargmann for the *odr-10* cDNA, and Dr. Kun Ling for assistance with confocal microscopy. This work was supported by a National Institutes of Health grant to M.M.B. and a PKD Foundation Research Fellowship to J. H. The Barr laboratory is a member of the Johns Hopkins Polycystic Kidney Disease Center for Excellence.

## REFERENCES

- Aguiari, G., *et al.* (2004). Deficiency of polycystin-2 reduces  $\text{Ca}^{2+}$  channel activity and cell proliferation in ADPKD lymphoblastoid cells. *FASEB J.* 18, 884–886.
- Arakaki, N., Nagao, T., Niki, R., Toyofuku, A., Tanaka, H., Kuramoto, Y., Emoto, Y., Shibata, H., Magota, K., and Higuti, T. (2003). Possible role of cell surface H(+)-ATP synthase in the extracellular ATP synthesis and proliferation of human umbilical vein endothelial cells. *Mol. Cancer Res.* 1, 931–939.
- Bae, T. J., *et al.* (2004). Lipid raft proteome reveals ATP synthase complex in the cell surface. *Proteomics.* 4, 3536–3548.
- Bakhtiar, N., Lai-Zhang, J., Yao, B., and Mueller, D. M. (1999). Structure/function of the beta-barrel domain of F1-ATPase in the yeast *Saccharomyces cerevisiae*. *J. Biol. Chem.* 274, 16363–16369.
- Bargmann, C. I., Hartwig, E., and Horvitz, H. R. (1993). Odorant-selective genes and neurons mediate olfaction in *C. elegans*. *Cell* 74, 515–527.
- Barr, M. M., DeModena, J., Braun, D., Nguyen, C. Q., Hall, D. H., and Sternberg, P. W. (2001). The *Caenorhabditis elegans* autosomal dominant polycystic kidney disease gene homologs *lov-1* and *pkd-2* act in the same pathway. *Curr. Biol.* 11, 1341–1346.
- Barr, M. M., and Sternberg, P. W. (1999). A polycystic kidney-disease gene homologue required for male mating behaviour in *C. elegans*. *Nature* 401, 386–389.
- Bateman, A., and Sandford, R. (1999). The PLAT domain: a new piece in the PKD1 puzzle. *Curr. Biol.* 9, R588–R590.
- Boletta, A., and Germino, G. G. (2003). Role of polycystins in renal tubulogenesis. *Trends Cell Biol.* 13, 484–492.
- Boyer, P. D. (1997). The ATP synthase—a splendid molecular machine. *Annu. Rev. Biochem.* 66, 717–749.
- Brenner, S. (1974). The genetics of *Caenorhabditis elegans*. *Genetics* 77, 71–94.
- Burwick, N. R., Wahl, M. L., Fang, J., Zhong, Z., Capaldi, R. A., Kenan, D. J., and Pizzo, S. V. (2004). An inhibitor of the F1 subunit of ATP synthase (IF1) modulates the activity of angiostatin on the endothelial cell surface. *J. Biol. Chem.* (in press).
- Chang, S. Y., Park, S. G., Kim, S., and Kang, C. Y. (2002). Interaction of the C-terminal domain of p43 and the alpha subunit of ATP synthase. Its functional implication in endothelial cell proliferation. *J. Biol. Chem.* 277, 8388–8394.



- Das, B., Mondragon, M. O., Sadeghian, M., Hatcher, V. B., and Norin, A. J. (1994). A novel ligand in lymphocyte-mediated cytotoxicity: expression of the beta subunit of H<sup>+</sup> transporting ATP synthase on the surface of tumor cell lines. *J. Exp. Med.* *180*, 273–281.
- Fraser, A. G., Kamath, R. S., Zipperlen, P., Martinez-Campos, M., Sohrmann, M., and Ahringer, J. (2000). Functional genomic analysis of *C. elegans* chromosome I by systematic RNA interference. *Nature* *408*, 325–330.
- Geng, L., *et al.* (1996). Identification and localization of polycystin, the PKD1 gene product. *J. Clin. Invest.* *98*, 2674–2682.
- Gonczy, P., *et al.* (2000). Functional genomic analysis of cell division in *C. elegans* using RNAi of genes on chromosome III. *Nature* *408*, 331–336.
- Granato, M., Schnabel, H., and Schnabel, R. (1994). *pha-1*, a selectable marker for gene transfer in *C. elegans*. *Nucleic Acids Res.* *22*, 1762–1763.
- Hanazawa, M., Mochii, M., Ueno, N., Kohara, Y., and Iino, Y. (2001). Use of cDNA subtraction and RNA interference screens in combination reveals genes required for germ-line development in *Caenorhabditis elegans*. *Proc. Natl. Acad. Sci. USA* *98*, 8686–8691.
- Hodgkin, J. (1983). Male phenotypes and mating efficiency in *Caenorhabditis elegans*. *Genetics* *103*, 43–64.
- Hooper, K. M., Unwin, R. J., and Sutters, M. (2003). The isolated C-terminus of polycystin-1 promotes increased ATP-stimulated chloride secretion in a collecting duct cell line. *Clin. Sci.* *104*, 217–221.
- Ibraghimov-Beskrovnaya, O., *et al.* (1997). Polycystin: in vitro synthesis, in vivo tissue expression, and subcellular localization identifies a large membrane-associated protein. *Proc. Natl. Acad. Sci. USA* *94*, 6397–6402.
- Igarashi, P., and Somlo, S. (2002). Genetics and pathogenesis of polycystic kidney disease. *J. Am. Soc. Nephrol.* *13*, 2384–2398.
- Kamath, R. S., *et al.* (2003). Systematic functional analysis of the *Caenorhabditis elegans* genome using RNAi. *Nature* *421*, 231–237.
- Kamath, R. S., Martinez-Campos, M., Zipperlen, P., Fraser, A. G., and Ahringer, J. (2001). Effectiveness of specific RNA-mediated interference through ingested double-stranded RNA in *Caenorhabditis elegans*. *Genome Biol.* *2*, 1–10.
- Kloda, A., Clements, J. D., Lewis, R. J., and Adams, D. J. (2004). Adenosine triphosphate acts as both a competitive antagonist and a positive allosteric modulator at recombinant N-methyl-D-aspartate receptors. *Mol. Pharmacol.* *65*, 1386–1396.
- Koushika, S. P., and Nonet, M. L. (2000). Sorting and transport in *C. elegans*: a model system with a sequenced genome. *Curr. Opin. Cell Biol.* *12*, 517–523.
- Leipzig, J. (2003). Control of epithelial transport via luminal P2 receptors. *Am. J. Physiol.* *284*, F419–F432.
- Li, N., Shaw, A. R., Zhang, N., Mak, A., and Li, L. (2004). Lipid raft proteomics: analysis of in-solution digest of sodium dodecyl sulfate-solubilized lipid raft proteins by liquid chromatography-matrix-assisted laser desorption/ionization tandem mass spectrometry. *Proteomics* *4*, 3156–3166.
- Liu, K. S., and Sternberg, P. W. (1995). Sensory regulation of male mating behavior in *Caenorhabditis elegans*. *Neuron* *14*, 79–89.
- Martinez, L. O., *et al.* (2003). Ectopic beta-chain of ATP synthase is an apolipoprotein A-I receptor in hepatic HDL endocytosis. *Nature* *421*, 75–79.
- Mello, C., and Fire, A. (1995). DNA transformation. *Methods Cell Biol.* *48*, 451–482.
- Moser, T. L., Kenan, D. J., Ashley, T. A., Roy, J. A., Goodman, M. D., Misra, U. K., Cheek, D. J., and Pizzo, S. V. (2001). Endothelial cell surface F1-F0 ATP synthase is active in ATP synthesis and is inhibited by angiotensin. *Proc. Natl. Acad. Sci. USA* *98*, 6656–6661.
- Moser, T. L., Stack, M. S., Asplin, I., Enghild, J. J., Hojrup, P., Everitt, L., Hubchak, S., Schnaper, H. W., and Pizzo, S. V. (1999). Angiotensin binds ATP synthase on the surface of human endothelial cells. *Proc. Natl. Acad. Sci. USA* *96*, 2811–2816.
- Pazour, G. J., San Agustin, J. T., Follit, J. A., Rosenbaum, J. L., and Witman, G. B. (2002). Polycystin-2 localizes to kidney cilia and the ciliary level is elevated in *ork* mice with polycystic kidney disease. *Curr. Biol.* *12*, R378–R380.
- Penefsky, H. S., and Cross, R. L. (1991). Structure and mechanism of FoF1-type ATP synthases and ATPases. *Adv. Enzymol. Relat. Areas Mol. Biol.* *64*, 173–214.
- Piano, F., Schetter, A. J., Morton, D. G., Gunsalus, K. C., Reinke, V., Kim, S. K., and Kempthues, K. J. (2002). Gene clustering based on RNAi phenotypes of ovary-enriched genes in *C. elegans*. *Curr. Biol.* *12*, 1959–1964.
- Rosenbaum, J. L., and Witman, G. B. (2002). Intraflagellar transport. *Nat. Rev. Mol. Cell Biol.* *3*, 813–825.
- Schwiebert, E. M., *et al.* (2002). Autocrine extracellular purinergic signaling in epithelial cells derived from polycystic kidneys. *Am. J. Physiol.* *282*, F763–F775.
- Schwiebert, E. M., and Zsembery, A. (2003). Extracellular ATP as a signaling molecule for epithelial cells. *Biochim. Biophys. Acta* *1615*, 7–32.
- Sengupta, P., Chou, J. H., and Bargmann, C. I. (1996). *odr-10* encodes a seven transmembrane domain olfactory receptor required for responses to the odorant diacetyl. *Cell* *84*, 899–909.
- Simmer, F., Moorman, C., Van Der Linden, A. M., Kuijk, E., Van Den Berghe, P. V., Kamath, R., Fraser, A. G., Ahringer, J., and Plasterk, R. H. (2003). Genome-Wide RNAi of *C. elegans* using the hypersensitive *rrf-3* strain reveals novel gene functions. *PLoS Biol.* *1*, E12.
- Simmer, F., Tijsterman, M., Parrish, S., Koushika, S. P., Nonet, M. L., Fire, A., Ahringer, J., and Plasterk, R. H. (2002). Loss of the putative RNA-directed RNA polymerase RRF-3 makes *C. elegans* hypersensitive to RNAi. *Curr. Biol.* *12*, 1317–1319.
- Sulston, J. E., Albertson, D. G., and Thomson, J. N. (1980). The *Caenorhabditis elegans* male: postembryonic development of nongonadal structures. *Dev. Biol.* *78*, 542–576.
- Tavemarakis, N., Wang, S. L., Dorovkov, M., Ryazanov, A., and Driscoll, M. (2000). Heritable and inducible genetic interference by double-stranded RNA encoded by transgenes. *Nat. Genet.* *24*, 180–183.
- Timmons, L., Court, D. L., and Fire, A. (2001). Ingestion of bacterially expressed dsRNAs can produce specific and potent genetic interference in *Caenorhabditis elegans*. *Gene* *263*, 103–112.
- Tsang, W. Y., and Lemire, B. D. (2002). Mitochondrial genome content is regulated during nematode development. *Biochem. Biophys. Res. Commun.* *291*, 8–16.
- Tsang, W. Y., Sayles, L. C., Grad, L. I., Pilgrim, D. B., and Lemire, B. D. (2001). Mitochondrial respiratory chain deficiency in *Caenorhabditis elegans* results in developmental arrest and increased life span. *J. Biol. Chem.* *276*, 32240–32246.
- Watnick, T., and Germino, G. (2003). From cilia to cyst. *Nat. Genet.* *34*, 355–356.
- White, J. G., Southgate, E., Thomson, J. N., and Brenner, S. (1986). The structure of the nervous system of the nematode *Caenorhabditis elegans*: the mind of a worm. *Phil. Trans. R. Soc. Lond.* *314*, 1–340.
- Wildman, S. S., Hooper, K. M., Turner, C. M., Sham, J. S., Lakatta, E. G., King, B. F., Unwin, R. J., and Sutters, M. (2003). The isolated cytoplasmic C-terminus of polycystin-1 prolongs ATP-stimulated chloride conductance through increased agonist stimulated calcium entry. *Renal Physiol.* *285*, 1168–1178.
- Wilson, P. D., Hovater, J. S., Casey, C. C., Fortenberry, J. A., and Schwiebert, E. M. (1999). ATP release mechanisms in primary cultures of epithelia derived from the cysts of polycystic kidneys. *J. Am. Soc. Nephrol.* *10*, 218–229.
- Yoder, B. K., Hou, X., and Guay-Woodford, L. M. (2002). The polycystic kidney disease proteins, polycystin-1, polycystin-2, polaris, and cystin, are co-localized in renal cilia. *J. Am. Soc. Nephrol.* *13*, 2508–2516.